Journal of Solid State Chemistry 233 (2016) 23–29

Contents lists available at ScienceDirect

Journal of Solid State Chemistry

journal homepage: www.elsevier.com/locate/jssc

Phase relations in the Na_2MoO_4–Cs_2MoO_4 and Na_2MoO_4–Cs_2MoO_4–$ZnMoO_4$ systems, crystal structures of $Cs_3Na(MoO_4)_2$ and $Cs_3NaZn_2(MoO_4)_4$

Evgeniya S. Zolotova [a], Zoya A. Solodovnikova [a], Vasiliy N. Yudin [a,b,*], Sergey F. Solodovnikov [a,b], Elena G. Khaikina [c,d], Olga M. Basovich [c], Iliya V. Korolkov [a], Irina Yu. Filatova [a]

[a] Nikolaev Institute of Inorganic Chemistry, Siberian Branch, Russian Academy of Sciences, Acad. Lavrentiev Ave. 3, Novosibirsk 630090, Russia
[b] Novosibirsk State University, Pirogov St. 2, Novosibirsk 630090, Russia
[c] Baikal Institute of Nature Management, Siberian Branch, Russian Academy of Sciences, Sakh'yanova St. 6, Ulan-Ude, 670047 Buryat Republic, Russia
[d] Buryat State University, Smolin St. 24a, Ulan-Ude, 670000 Buryat Republic, Russia

ARTICLE INFO

Article history:
Received 25 June 2015
Received in revised form
28 September 2015
Accepted 4 October 2015

Keywords:
Cesium
Sodium
Zinc
Molybdates
Phase diagram
Aliovalent substitution
Vacancy solid solution
Crystal structure
Cation disorder

ABSTRACT

The phase diagram of the Na_2MoO_4–Cs_2MoO_4 system was reinvestigated and a new intermediate compound, $Cs_3Na(MoO_4)_2$, melting incongruently at 510 °C was found. Its crystal structure (a=6.3461(2), c=8.2209(3) Å, sp. gr. $P\bar{3}m1$, Z=1, R=0.0131) belongs to the glaserite type. Taking into account these data, the subsolidus phase relations of the system Na_2MoO_4–Cs_2MoO_4–$ZnMoO_4$ was studied at 420 °C. The filling vacancies in the tetrahedral Zn position of the $Cs_6Zn_5(MoO_4)_8$ structure (sp. gr. $I\bar{4}3d$, Z=2) following the scheme $Zn^{2+}+\square \rightarrow 2Na^{+}$ was established to result in the continuous solid solution $Cs_6Zn_{5-x}\square_{1-x}Na_{2x}(MoO_4)_8$ ($0 \le x \le 1$). With increasing the x value, the cubic lattice parameter of the solid solution increases linearly while its melting point decreases that testifies to destabilization of the $Cs_6Zn_5(MoO_4)_8$ structure by a progressive Na^{+} insertion. In the structure of $Cs_3NaZn_2(MoO_4)_4$ (a=12.3134(1) Å, R=0.0121), MoO_4 and $(Zn_{2/3}Na_{1/3})O_4$ tetrahedra share corners to form an open 3D framework. The cesium ions are disordered around the centers of the cuboctahedral cavities of the framework to form "clusters" of the central Cs(1) and four disordered Cs(2) positions.

1. Introduction

By now, numerous double molybdates have been synthesized, among which $AR(MoO_4)_2$ (A=Li–Cs; R=Ln, Y, Bi) are of great importance as laser hosts, phosphors, ferroelectrics, and other technically vital materials [1,2]. Some double molybdates of alkali and bivalent metals, such as $A_2Pb(MoO_4)_2$ (A=K, Rb, Cs), $A_4Zn(MoO_4)_3$ (A=K, Rb), and $Cs_2Zn(MoO_4)_2$ possess ferroelastic properties [3] caused by specific crystal-chemical features of "elastoactive" Pb^{2+} and Zn^{2+} cations [4]. In particular, distortive phase transitions and ferroelastic properties of $A_4Zn(MoO_4)_3$ (A=K, Rb) were explained by lowering the zinc coordination from the trigonal bipyramidal to the tetrahedral one [5].

A tendency of zinc to lower its coordination and to adopt tetrahedral oxygen environment unlike other bivalent medium-sized cations [6] originates the unique composition and structure of cubic $Cs_6Zn_5(MoO_4)_8$ (sp. gr. $I\bar{4}3d$, Z=2) with vacancies in the tetrahedral zinc position, $Cs_3(Zn_{5/6}\square_{1/6})_3(MoO_4)_4$ [7,8]. This opens a principal opportunity for filling the vacancies by means of proper aliovalent interstitial substitutions, for example, $Zn^{2+}+\square \rightarrow 2Li^{+}$. Such an opportunity was realized in the systems Li_2MoO_4–A_2MoO_4–$MMoO_4$ (A=Rb, Cs; M=Co, Zn) where we have revealed cubic phases $A_3LiZn_2(MoO_4)_4$ (A=Rb, Cs) and $Cs_3LiCo_2(MoO_4)_4$ [9,10] with a statistical distribution of Li^{+} and M^{2+} cations in the tetrahedral zinc position of the $Cs_6Zn_5(MoO_4)_8$ structure. These triple molybdates may be considered as promising solid lithium-ion conductors. The corresponding investigations are in progress and the results will be published elsewhere.

The main aim of this work was the preparation of sodium containing analog of $Cs_3LiZn_2(MoO_4)_4$ and study of the phase formation in the Na_2MoO_4–Cs_2MoO_4–$ZnMoO_4$ system along with verifying the possibility of a gradual insertion of sodium ions into vacancies of the tetrahedral zinc position in the $Cs_6Zn_5(MoO_4)_8$ structure.

* Corresponding author. Fax: +7 383 309489.
E-mail address: yuvasilij@yandex.ru (V.N. Yudin).

http://dx.doi.org/10.1016/j.jssc.2015.10.008
0022-4596/

The binary systems bounding the ternary system Na_2MoO_4–Cs_2MoO_4–$ZnMoO_4$ are described in the literature [11–16]. According to data of [11,12], the Na_2MoO_4–Cs_2MoO_4 system is eutectic with boundary solid solutions. In the Cs_2MoO_4–$ZnMoO_4$ system, three compounds are formed, $Cs_4Zn(MoO_4)_3$ existing in the range 320–440 °C and decomposing in the solid state, $Cs_2Zn(MoO_4)_2$ and $Cs_6Zn_5(MoO_4)_8$ melting incongruently [7,8,13]. In the Na_2MoO_4–$ZnMoO_4$ system, three phases were found to exist, monoclinic $Na_{2+2x}Zn_{1-x}(MoO_4)_2$ ($x \approx 0.1$), orthorhombic $Na_{2-2y}Zn_{2+2y}(MoO_4)_3$ ($y \approx 0.1$), and triclinic $Na_2Zn_4(MoO_4)_5$ [14–16]. However, the crystal structure determinations of the latter phase gave other controversial compositions, $Na_2Zn_5(MoO_4)_6$ [17] or $Na_{0.5}Zn_{2.75}(MoO_4)_3$ [18].

In view of incomplete data on the binary systems bounding the Na_2MoO_4–Cs_2MoO_4–$ZnMoO_4$ system, we have studied again the Na_2MoO_4–Cs_2MoO_4 and Na_2MoO_4–$ZnMoO_4$ systems and revised the compositions of nonstoichiometric sodium–zinc molybdates and the *T*–*x* phase diagram of the Na_2MoO_4–Cs_2MoO_4 system.

2. Experimental section

2.1. Preparing samples

Commercially available MoO_3, Cs_2CO_3, $Na_2MoO_4 \cdot 2H_2O$, and ZnO (all analytical grade) were taken as initial materials. Anhydrous Na_2MoO_4 was obtained by calcination of the corresponding crystalline hydrate, $Na_2MoO_4 \cdot 2H_2O$, at 550–600 °C. Simple molybdates Cs_2MoO_4 and $ZnMoO_4$ were prepared by annealing the appropriate stoichiometric mixtures of Cs_2CO_3, ZnO, and MoO_3 at 500–600 °C for 50 h. Cesium dimolybdate, $Cs_2Mo_2O_7$, was obtained at 450 °C for 50 h. Double molybdates in the Na_2MoO_4–$ZnMoO_4$ and Cs_2MoO_4–$ZnMoO_4$ systems were synthesized from stoichiometric mixtures of the corresponding simple molybdates at 420–700 °C for 50–200 h. The powder X-ray diffraction patterns of all compounds prepared were in a good agreement with literature data.

The monophase sample of $Cs_3NaZn_2(MoO_4)_4$ isostructural to $Cs_6Zn_5(MoO_4)_8$ was obtained by annealing the corresponding mixture of Cs_2MoO_4, Na_2MoO_4 and $ZnMoO_4$ at 400–550 °C for 100 h. Colorless isometric $Cs_3NaZn_2(MoO_4)_4$ crystals sized up to 0.5 mm were prepared from a melted polycrystalline monophase sample after holding the melt for 24 h at 560 °C followed by cooling to 400 °C at the rate of 3 deg h^{-1}.

Colorless hexagonal plate crystals of $Cs_3Na(MoO_4)_2$ up to 0.5 mm in diameter were obtained from a polycrystalline monophase sample after its cooling in the range 520–400 °C at the rate of 10 deg h^{-1} followed by switching off the furnace with the sample. Under a polarizing microscope, the crystals were found to be uniaxial at room temperature.

2.2. Study of phase formation and phase equilibria

The reaction mixtures for studying phase relations and constructing the *T*–*x* phase diagram of the Na_2MoO_4–Cs_2MoO_4 system were taken with step of 5 mol%; in the vicinity of the initial components and the compositions of the expected intermediate phases, the step being 1–2.5 mol%. The samples were annealed at 350–450 °C for 100–250 h.

The subsolidus phase relations of the Cs_2MoO_4–Na_2MoO_4–$ZnMoO_4$ system were determined using the "intersecting joins" method [19,20]. In order to determine quasi binary joins in this system and its triangulation, we have to know the phase compositions of the annealed samples corresponding to the intersection points of the joins originating from the composition points of all components and binary compounds of the system. Inspecting all intersection points of the joins in the ternary system allow us to reveal all quasi binary joins provided that no ternary compounds exist in the system.

According to [7,8,13–16], the Cs_2MoO_4–Na_2MoO_4–$ZnMoO_4$ system contains six double molybdates in the boundary systems, therefore the number of intersection points of the corresponding joins is rather high, making the application of the "intersecting joins" method very laborious. The modified method of "significant points" [20] was applied for making our job easier. The method allows selecting the minimum required set of intersections points of the joins ("significant points") sufficient for constructing the unambiguous triangulation providing that all compositions of binary and ternary compounds in the ternary system are known. Without knowledge of the compositions of the ternary compounds, we can fix their presence in the significant points which are within the secondary systems involving such compounds to estimate their existence regions in the system.

Samples corresponding to 9 significant points of the Cs_2MoO_4–Na_2MoO_4–$ZnMoO_4$ system, were prepared from the starting binary compounds forming this couple of intersecting joins, two samples were prepared for each significant point. The samples were annealed at 380–420 °C at least 200 h with intermittent grindings of 1 – 2 times a day. The temperature was raised by 5–20 °C for 20 h of annealing. The attainment of equilibrium was tested by XRD.

At the next stage, we examined the possibility of forming the boundary solid solutions and triple molybdates previously undetected in the system. The joins Na_2MoO_4–$Cs_2Zn(MoO_4)_2$, Na_2MoO_4–$Cs_6Zn_5(MoO_4)_8$, Na_2MoO_4–$Cs_3NaZn_2(MoO_4)_4$ and partially $Cs_3Na(MoO_4)_2$–$ZnMoO_4$ (over 66.7 mol% $ZnMoO_4$) were investigated in more detail with the step of 2.5–10 mol%. The samples were annealed at 400–420 °C for at least 150 h. To study the possibility of gradual inserting the sodium cations into the $Cs_6Zn_5(MoO_4)_8$ structure with the formation of a vacancy solid solution, we also prepared the samples of the join $Cs_6Zn_5(MoO_4)_8$–$Cs_3NaZn_2(MoO_4)_4$ with a step of 10 mol% using the corresponding mixtures of monophase $Cs_6Zn_5(MoO_4)_8$ and $Cs_3NaZn_2(MoO_4)_4$ annealed at 420 °C for 200 h. The samples prepared were characterized by XRD and differential thermal analysis (DTA).

For searching ternary molybdates, we also used spontaneous crystallization of different melted mixtures of Cs_2MoO_4–Na_2MoO_4–$ZnMoO_4$ system, sometimes with $Cs_2Mo_2O_7$ as a flux. Homogenization temperatures were 500–600 °C, the cooling rates were 3–5 deg h^{-1}.

2.3. X-ray powder diffraction and thermal analysis

XRD patterns were taken on a DRON-SEIFERT-RM4 diffractometer (CuK_α radiation, Ni filter, 2θ range of 5–60°) at room temperature. The samples crushed in heptane were put in a 100 μm thick layer on a polished side of a standard quartz holder. A polycrystalline Si sample ($a = 5.43075$ Å) prepared in such a way was used as an external standard. The unit cell parameters were refined by using the PowderCell 2.4 program. The peak profiles were described by the asymmetric Lorentz function in the range of $2\theta = 15$–57° [21].

Thermal analysis was performed in air using a MOM OD-103 derivatograph (Pt–Pt/Rh thermocouples, Pt crucibles, heating, cooling and DTA curves, Al_2O_3 as reference substance, heating and cooling rates 10 °C min^{-1}).

2.4. Single-crystal structure analysis

Fragments of $Cs_3Na(MoO_4)_2$ and $Cs_3NaZn_2(MoO_4)_4$ crystals were selected for X-ray structure analysis. Single-crystal XRD data were collected with graphite-monochromated MoKα radiation

(λ=0.71073 Å) on a Bruker-Nonius X8 Apex CCD area-detector diffractometer at room temperature using φ-scans with $\Delta\varphi$=0.5°. Data processing was accomplished using the SAINT program; an absorption correction was applied with the SADABS program [22].

$Cs_3Na(MoO_4)_2$ structure was solved by direct methods in the sp. gr. $P\bar{3}m1$ and refined by full-matrix least-squares method on F^2 in anisotropic approximation with the SHELX97 program package [22].

The structure of $Cs_3NaZn_2(MoO_4)_4$ was determined in the sp. gr. $I\bar{4}3d$ in anisotropic approximation for all atoms and basically confirmed data obtained for isostructural $Cs_6Zn_5(MoO_4)_8$ [7,8], $Rb_3LiZn_2(MoO_4)_4$, and $Cs_3LiCo_2(MoO_4)_4$ [8]. The refinement of $Cs_3NaZn_2(MoO_4)_4$ structure with the (Zn, Na) position content as (2Zn+Na)/3 and the cesium atom in the 12b Wyckoff position as in [7,8] resulted in R=0.0299 with the residual electron density peaks of 2.2 e/Å^3 near the cesium position. This was evidence of disordering the cesium cations caused by their displacement from the special position to a general one. However, the refinement of the structure with cesium displaced from the 12*b* position resulted in "gathering" the split cesium atoms in this special position again. A further refinement with two close cesium positions, 12*b* and 48*e*, resulted in R=0.0121 and reasonable atomic displacement parameters and interatomic distances.

The crystal data and final results of the X-ray structure analysis for $Cs_3Na(MoO_4)_2$ and $Cs_3NaZn_2(MoO_4)_4$ are summarized in Table 1.

3. Results and discussion

Upon studying the phase formation in the system Na_2MoO_4–Cs_2MoO_4–$ZnMoO_4$, we have used data of [13] on the boundary Cs_2MoO_4–$ZnMoO_4$ system and results of our re-investigations of the Na_2MoO_4–$ZnMoO_4$ and Na_2MoO_4–Cs_2MoO_4 systems.

Our XRD data on the Na_2MoO_4–$ZnMoO_4$ system samples annealed at 420 °C for 150 h revealed formation of two nonstoichiometric double molybdates: monoclinic $Na_{4-2x}Zn_{1+x}(MoO_4)_3$ ($0.1 \le x \le 0.4$) with the structure of alluaudite $(Na,Mn^{2+},Ca)(Mn^{2+},Mg,Li)(Fe^{3+},Mg)_2(PO_4)_3$ [23] and orthorhombic

Table 1
Crystal data and structure refinement details for $Cs_3Na(MoO_4)_2$ and $Cs_3NaZn_2(MoO_4)_4$

Formula	$Cs_3Na(MoO_4)_2$	$Cs_3NaZn_2(MoO_4)_4$
Formula weight (g/mol)	741.60	2293.91
Crystal system	trigonal	cubic
Space group	$P\bar{3}m1$	$I\bar{4}3d$
Unit cell dimensions	a=6.3461(2) Å	a=12.3134(1) Å
V (Å^3); Z	c=8.2209(3) Å	
	286.72(2) / 1	1866.96(3) / 4
Calculated density (g cm^{-3})	4.295	4.239
Crystal size, mm	0.04 × 0.04 × 0.03	0.16 × 0.10 × 0.05
μ(MoK$_\alpha$), mm^{-1}	11.620	10.980
θ range (deg) for data collection	2.48–28.31	4.05–32.47
Miller index ranges	$-6 \le h \le 8$, $-8 \le k \le 8$, $-10 \le l \le 9$	$-12 \le h \le 18$, $-18 \le k \le 18$, $-13 \le l \le 18$
Reflections collected/unique	2786/307 [R(int)= 0.0238]	8921/569 [R(int)= 0.0197]
No. of variables	21	30
Goodness-of-fit on F^2 (GOF)	1.169	1.152
Final R indices [$I > 2\sigma(I)$]	$R(F)$=0.0131, $wR(F^2)$=0.0311	$R(F)$=0.0121, $wR(F^2)$=0.0305
R indices (all data)	$R(F)$=0.0132, $wR(F^2)$=0.0311	$R(F)$=0.0124, $wR(F^2)$=0.0306
Extinction coefficient	0.015(1)	none
Largest difference peak/hole (e Å^{-3})	0.342/−0.704	0.343/−0.659

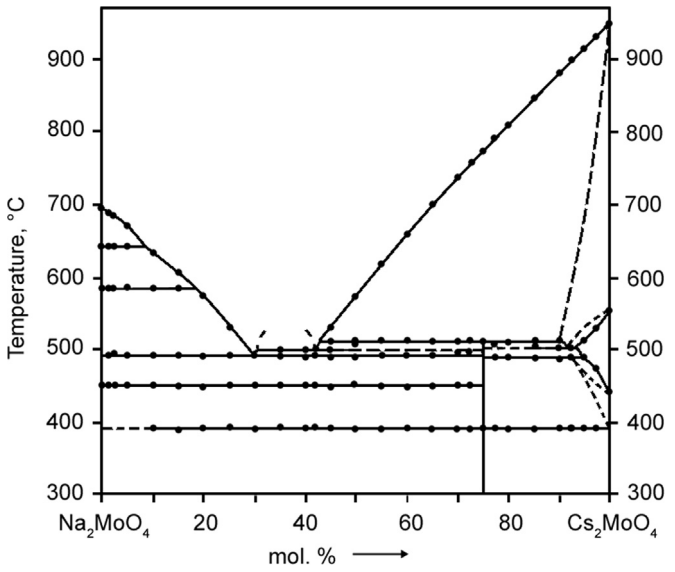

Fig. 1. The T–x phase diagram of the Na_2MoO_4–Cs_2MoO_4 system.

$Na_{2-2y}Zn_{2+y}(MoO_4)_3$ ($0.1 \le y \le 0.2$) of the lyonsite α-$Cu_3Fe_4(VO_4)_6$ type [24]. It was established that the triclinic compound $Na_2Zn_4(MoO_4)_5$ found in [14–16] and isostructural to $Na_2Mg_5(MoO_4)_6$ [17] or $Na_{0.5}Zn_{2.75}(MoO_4)_3$ [18] has the real composition $Na_{2-2z}Zn_{2+z}(MoO_4)_3$ ($0.1 \le z \le 0.4$) and exists above 550 °C only. The detailed results of studying the phase formation and the structure of intermediate phases of the Na_2MoO_4–$ZnMoO_4$ system will be published elsewhere.

3.1. *T–x phase diagram of Na_2MoO_4–Cs_2MoO_4 system*

The T–x phase diagram of the Na_2MoO_4–Cs_2MoO_4 system was constructed from DTA and XRD results for sintered samples (Fig. 1). In contrast to [11,12], wherein the system is considered as an eutectic that with the boundary solid solutions, we found the intermediate compound $Cs_3Na(MoO_4)_2$; its composition was confirmed by single crystal X-ray analysis. The extension of the solid solution based on Cs_2MoO_4 reaches 10 mol%, no noticeable homogeneity regions on the basis of Na_2MoO_4 polymorphs were fixed. The eutectic melts at 490 °C and contains about 70 mol% of Na_2MoO_4. The presence of an extended horizontal line on the liquidus in the range of 58–70 mol% of Na_2MoO_4 seems to be caused by an aliquation of the liquid phase.

According to XRD data, a noticeable interaction between Na_2MoO_4 and Cs_2MoO_4 begins at 250 °C. Solid state synthesis of $Cs_3Na(MoO_4)_2$ was carried out at 420 °C for 150 h. The diffractogram of the sintered sample of $Cs_3Na(MoO_4)_2$ is in a good agreement with the theoretical one calculated from the single crystal X-ray structure data (see below). The double molybdate has a reversible polymorphic transition at 390 °C and melts peritectically at 510 °C. Additional annealing of $Cs_3Na(MoO_4)_2$ sample at 350 °C gave no rise to a noticeable changing of the diffraction pattern, which may be explained by a negligible deformation of the structure below the polymorphic transition at 390 °C.

The formula of $Cs_3Na(MoO_4)_2$ is analogous to the compositions of $M_3Na(MoO_4)_2$ (M=K, Rb) structurally studied in [25,26]. Perhaps, these compounds are the end members of extended solid solutions reported in the systems Na_2MoO_4–K_2MoO_4 (about 40–70 mol% of K_2MoO_4) [27] and Na_2MoO_4–Rb_2MoO_4 (50–67 mol% of Rb_2MoO_4) [28]. The absence of a homogeneity region for $Cs_3Na(MoO_4)_2$ may be associated with a considerable difference between Cs^+ and Na^+ ionic radii. It should be also noted that $K_3Na(MoO_4)_2$ has a reversible phase transition at 420 °C [25]

Table 2
Selected interatomic distances (Å) for $Cs_3Na(MoO_4)_2$.

Mo-tetrahedron		**Na-octahedron**	
Mo–O(1)	1.771(2) × 3	(Na)–O(1)	2.537(2) × 6
–O(2)	1.732(6)		
< Mo(1)–O >	1.761		
Cs(1)-polyhedron		**Cs(2)-polyhedron**	
Cs(1)–O(1)	3.245(2) × 6	Cs(2)–O(1)	3.181(1) × 6
–O(2)	3.669(1) × 6	–O(1′)	3.411(2) × 3
		–O(2)	2.891(6)
< Cs(1)–O >	3.457	< Cs(2)–O >	3.221

whereas no such transition was found in $Rb_3Na(MoO_4)_2$ [26]. Perhaps, this compound undergoes phase transitions below room temperature.

3.2. Crystal structure of $Cs_3Na(MoO_4)_2$

The atomic coordinates, equivalent isotropic displacement parameters and selected interatomic distances for $Cs_3Na(MoO_4)_2$ and are listed in Table S1 and Table 2. In the structure, Mo, Cs (2) and O(1) atoms occupy the 2d positions (3*m* site symmetry); Na and Cs(1) (both with $\bar{3}m$ site symmetry) are in 1*a* and 1*b*, respectively, and O(2) atoms are located in general 12*j* sites. The molybdenum atoms are tetrahedrally coordinated by oxygen atoms with the distances Mo–O 1.723(14)–1.771(5) Å. The sodium atoms are located in nearly regular octahedra with the equal Na–O bond lengths 2.541(5) Å.

The structure of $Cs_3Na(MoO_4)_2$ belongs to the glaserite type, $K_3Na(SO_4)_2$ [29,30]. The basic fragment of the structure is the layer of the alternating MoO_4 tetrahedra and NaO_6 octahedra connected by oxygen vertices (Fig. 2(a)). The layers are separated by interlayers of $Cs(1)O_{12}$ icosahedra and $Cs(2)O_{10}$ polyhedra with the Cs–O distances of 2.900(14)–3.670(1) Å (Fig. 2(b)). Each MoO_4 tetrahedron links three $Cs(1)O_{12}$, five $Cs(2)O_{10}$ polyhedra, and three NaO_6 octahedra. Each NaO_6 octahedron shares faces with two adjacent $Cs(1)O_{12}$ and six $Cs(2)O_{10}$ polyhedra while each $Cs(2)O_{10}$ polyhedron connects with three NaO_6 octahedra and three $Cs(2)O_{10}$ polyhedra through common faces.

The double molybdate $Rb_3Na(MoO_4)_2$ [26] is isostructural to $Cs_3Na(MoO_4)_2$ while $K_3Na(XO_4)_2$ (X=Mo, W) have monoclinically distorted structures (sp. gr. *C*2/*c*) with the transformation matrices $-1\ -1\ 0\ /\ 1\ -1\ 0\ /\ 0\ 0\ 2$ from the primitive trigonal unit cells to the *C*-centered pseudo-orthorhombic ones [25]. Analogous monoclinic structures were also found for low-temperature modifications of $K_3Na(XO_4)_2$ (X=Se, Cr) which have ferroelastic properties [26]. Evidently, the trigonal structure of $Cs_3Na(MoO_4)_2$ studied by us, refers to the high-temperature form of the compound.

3.3. Phase relations in Na_2MoO_4–Cs_2MoO_4–$ZnMoO_4$ system

From XRD data of the prepared samples corresponding to 9 significant points of the Cs_2MoO_4–Na_2MoO_4–$ZnMoO_4$ system (Fig. S1), quasi binary joins of the system were pre-determined. For each significant point, the same phase compositions were obtained for two pairs of the starting compounds of the intersecting joins. Powder XRD analysis of quasi binary joins showed that noticeable ranges of solid solutions exist for the join $Cs_2Zn(MoO_4)_2$–Na_2MoO_4 (up to 10 mol% of Na_2MoO_4), as well as for the joins connecting $Cs_3NaZn_2(MoO_4)_4$ with $Na_{3.8}Zn_{1.1}(MoO_4)_3$, $Na_{3.2}Zn_{1.4}(MoO_4)_3$, $Na_{1.8}Zn_{2.1}(MoO_4)_3$, $Na_{1.6}Zn_{2.2}(MoO_4)_3$ (about 5 mol% of $Cs_3NaZn_2(MoO_4)_4$), Na_2MoO_4, $Cs_2Zn(MoO_4)_2$ (about 10 mol% of $Cs_3NaZn_2(MoO_4)_4$) and $ZnMoO_4$ (about 20 mol% of $Cs_3NaZn_2(MoO_4)_4$).

According to XRD data, all the synthesized samples of the quasi binary join $Cs_6Zn_5(MoO_4)_8$–$Cs_3NaZn_2(MoO_4)_4$ are monophase and isostructural to $Cs_6Zn_5(MoO_4)_8$. Thus, the continuous solid solution $Cs_6Zn_{5-x}Na_{2x}(MoO_4)_8$ ($0 \le x \le 1$) forms on the join due to the aliovalent interstitial substitution $Zn^{2+} + \square \rightarrow 2\ Na^{+}$. The lattice parameter increases on this join (Table 2S and Fig. 3) in accordance with the Vegard's law and the tetrahedral ionic radii of Zn^{2+} and Na^{+} (0.74 and 1.13 Å, respectively) [31]. The cubic unit cell parameter of the studied $Cs_3NaZn_2(MoO_4)_4$ single crystal (Table 1) agrees well with the lattice parameter measured for the corresponding powder sample (Table S2). At the same time, with increasing the sodium content, the melting point of $Cs_6Zn_{5-x}Na_{2x}(MoO_4)_8$ solid solution (Table S2) decreases monotonically. By this is meant that the addition of Na^{+} has a destabilizing effect on the $Cs_6Zn_5(MoO_4)_8$ structure. The members of the solid solution series $Cs_6Zn_{5-x}Na_{2x}(MoO_4)_8$ ($0 \le x \le 1$) were found to melt incongruently and partially decompose into simple constituent molybdates.

The subsolidus triangulation of the Na_2MoO_4–Cs_2MoO_4–$ZnMoO_4$ system at 420 °C is shown in Fig. 4. The phase relations exclude triclinic phase $Na_{2-2z}Zn_{2+z}(MoO_4)_3$ ($0.1 \le z \le 0.4$) existing above 550 °C and include $Cs_4Zn(MoO_4)_3$ decomposing in the solid state above 440 °C to yield $Cs_2Zn(MoO_4)_2$ and Cs_2MoO_4. Above 440 °C, the number of the secondary systems is reduced by one. In accordance with the homogeneity ranges found for quasi binary joins involving $Cs_3NaZn_2(MoO_4)_4$, the existence region of the solid solution passes the limits of the $Cs_6Zn_5(MoO_4)_8$–$Cs_3NaZn_2(MoO_4)_4$ join and forms the 2D area (Fig. 4). This may be associated with both the complex isomorphism (Zn, Na, □) in the tetrahedral zinc position in the $Cs_6Zn_5(MoO_4)_8$ structure and a partial substitution (Cs, Na).

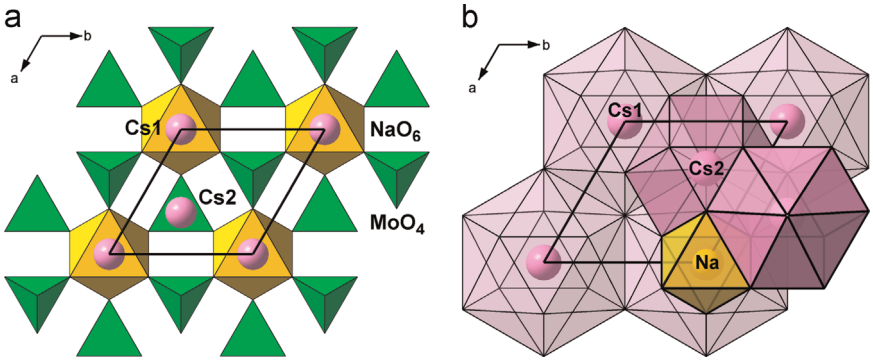

Fig. 2. The projection of $Cs_3Na(MoO_4)_2$ structure on (001) plane: (a) a layer of MoO_4 tetrahedra and NaO_6 octahedra; (b) a fragment of the layer of $Cs(1)O_{12}$ icosahedra and $Cs(2)O_{10}$ polyhedra with an inscribed NaO_6 octahedron.

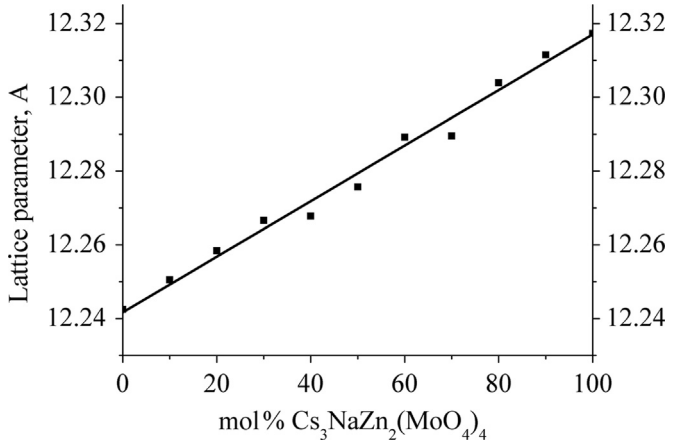

Fig. 3. The dependence of the cubic unit cell parameter on the composition of the continuous solid solution $Cs_6Zn_5(MoO_4)_8$–$Cs_3NaZn_2(MoO_4)_4$.

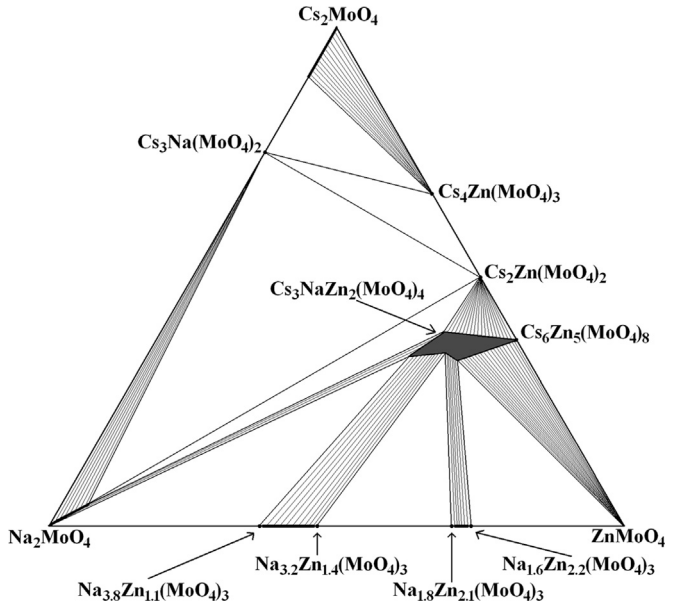

Fig. 4. The triangulation of the subsolidus field of Cs_2MoO_4–Na_2MoO_4–$ZnMoO_4$ system at 420 °C.

3.4. *Crystal structure of $Cs_3NaZn_2(MoO_4)_4$*

The atomic coordinates, equivalent isotropic displacement parameters and selected interatomic distances for $Cs_3NaZn_2(MoO_4)_4$ are listed in Table S3 and Table 3. In the structure,"atoms" M=($Zn_{2/3}Na_{1/3}$) occupy the 12a position ($\bar{4}$ site symmetry); Mo atoms are at three-fold axes (16c) and Cs(1) atoms are in the 12*b* position with the site symmetry $\bar{4}$. The "split" (disordered) Cs (2) atoms are located in general 48*e* sites. The oxygen atoms, O (1) and O(2), are in the special 16*c* and general 48*e* positions, respectively, to form the tetrahedral environment of (Zn, Na) and Mo atoms. The Cs(1) atom in the 12b has a nearly regular 12-fold cuboctahedral coordination, whereas the range of the Cs–O bond lengths for Cs(2) in the 48*e* are much wider (Table 3) within the same coordination sphere.

Four vertices of the MoO_4 tetrahedra and three corners of the (Zn,Na)O_4 tetrahedra link to each other to form an open 3D framework (Fig. 5(a)). The Cs^+ ions are located in large cavities of the tetrahedral framework. A "cage" of the framework with the alternating MoO_4 and (Zn,Na)O_4 tetrahedra around Cs(1) and Cs (2) is shown in Fig. 5(b). In the cage, the characteristic eight-membered tetrahedral ring (numbers 1–8) with four attached

Table 3
Selected interatomic distances (Å) for $Cs_3NaZn_2(MoO_4)_4$.

Mo-tetrahedron	**(Zn, Na)-tetrahedron**
Mo–O(1)1.782(2) × 3	(Zn, Na)–O(1)1.987(2) × 4
–O(2)1.719(3)	
< Mo(1)–O > 1.762	
Cs(1)-polyhedron	**Cs(2)-polyhedron**
Cs(1)–O(1)#13.254(2)	Cs(2)–O(1)#23.13(2)
–O(1)#23.254(2)	–O(1)#33.28(2)
–O(1)#33.254(2)	–O(1)#83.28(2)
–O(1)#43.254(2)	–O(1)#93.29(2)
–O(2)#53.370(1)	O(2)#63.29(3)
–O(2)#23.370(1)	–O(1)#13.30(1)
–O(2)#63.370(1)	–O(2)#23.32(1)
–O(2)#43.370(1)	–O(1)#43.32(3)
–O(1)#73.390(2)	–O(2)#43.38(2)
–O(1)#83.390(2)	–O(1)#103.49(2)
–O(1)#9 3.390(2)	–O(1)#103.49(2)
–O(1)#103.390(2)	–O(1)#73.52(2)
< Cs(1)–O > 3.338	< Cs(2)–O > 3.34

Symmetry codes: #1 $x+3/4, z-1/4, y-1/4$; #2 $-x+1, y-1/2, -z+1/2$; #3 $x+3/4, -z+1/4, -y+3/4$; #4 $-x+1, -y+1/2, z$; #5 $y+3/4, -x+1/4, -z+3/4$; #6 $y+3/4, x-1/4, z-1/4$; #7 $z+1/2, -x+1/2, -y+1$; #8 $z+1/2, x-1/2, y-1/2$; #9 $-z+5/4, -y+3/4, x-1/4$; #10 $-z+5/4, y-3/4, -x+3/4$.

terminate MoO_4 tetrahedra (9–12) is manifested. Each (Zn,Na)O_4 tetrahedron takes part in four rings, whereas each MoO_4 tetrahedron connects three rings. The distance (Zn, Na)–O 1.987(2) Å in $Cs_3NaZn_2(MoO_4)_4$ is close to bond lengths Zn–O 1.975(8) Å in $Cs_6Zn_5(MoO_4)_8$ [8] and 1.858–2.038 Å (average 1.95 Å) in $K_4Zn(MoO_4)_3$ [32].

The main difference of the $Cs_3NaZn_2(MoO_4)_4$ structure from those of $Cs_6Zn_5(MoO_4)_8$ [7,8], $Rb_3LiZn_2(MoO_4)_4$, and $Cs_3LiCo_2(MoO_4)_4$ [9] is the "splitting" of the cesium positions. Perhaps, this is caused by a local non-equivalence of four nearest ($Zn_{2/3}Na_{1/3}$) positions of the $Cs_3NaZn_2(MoO_4)_4$ structure inducing the shifts of the cesium cations from the special positions towards sodium sites to compensate charge disbalances. The assumption is confirmed by the arrangement of the "shifted" cesium atoms on the line connecting the Cs (12b) and (Zn, Na) positions (Fig. 5(b)). The Cs(1) cation positioning in the 12*b* appears to fit its environment by four nearest zinc atoms.

One more example of a similar tetrahedral framework consisting of the $(Li_{1/3}\square_{2/3})O_4$ and SO_4 tetrahedra was found in proton conductor $Cs_3Li(DSO_4)_4$ [33]. The another "polymorphous modification" of the framework occurs in the structures of mayenite $12CaO \cdot 7Al_2O_3$ [34] and related compounds $11CaO \cdot 7Al_2O_3 \cdot CaF_2$ [35], wadalite $Ca_6Al_5Si_2O_{16}Cl_3$ [36] and $Na_6Zn_3(AsO_4)_4 \cdot 3H_2O$ [37] wherein the terminal vertices of the Al(Si)O_4 or AsO_4 tetrahedra are opposite-directed along the threefold axes compared to the MoO_4 tetrahedra in the $Cs_6Zn_5(MoO_4)_8$ family.

Unlike Zn^{2+} and Li^+ ions, the tetrahedral coordination is non-typical for the sodium ions with their usual CN 6 and higher coordinations. Rare examples of the tetrahedral coordination of the sodium atoms in molybdates are provided by the structures of $Na_5Ln(MoO_4)_4$ (Ln=La–Lu) [38] with the Na–O distances of 2.42–2.48 Å, significantly longer than the (Zn,Na)–O bond lengths in $Cs_3NaZn_2(MoO_4)_4$. Further examples of the tetrahedral sodium coordination in oxides are Na_2O (Na–O 2.40 Å) [39], the β-$NaFeO_2$ type phases [40,41] and those of the Na_2ZnSiO_4 type [42,43] with the Na–O bonds no less than 2.3 Å. Hence, the effective vacancy size in the $Cs_6Zn_5(MoO_4)_8$ structure is too small for the Na^+ cation to be arranged therein easily. This creates the steric strain in $Cs_6Zn_{5-x}Na_{2x}(MoO_4)_8$ ($0 \le x \le 1$) that grows with the sodium content resulting in the thermal destabilization of the solid

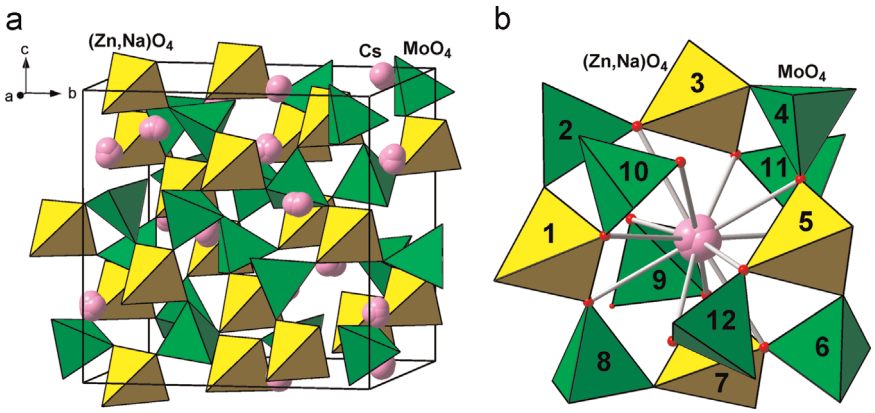

Fig. 5. Crystal structure of $Cs_3NaZn_2(MoO_4)_4$: (a) a general view; (b) a tetrahedral cage around Cs(1) and Cs(2). The eight-membered ring is indicated by the tetrahedra labeled 1–8; attached tetrahedra numbered 9–12.

solution.

The lithium cations exert the opposite effect on the $Cs_6Zn_5(MoO_4)_8$ structure, as confirmed by increasing the thermal stability in the row $Cs_3NaZn_2(MoO_4)_4$ – $Cs_6Zn_5(MoO_4)_8$ – $Cs_3LiZn_2(MoO_4)_4$ with melting points 510, 650, and 740 °C, respectively. This stabilizing impact of Li^+ ions on the structure correlates well with the tetrahedral ionic radii of Li^+ (0.73 Å), Zn^{2+} (0.74 Å), and Na^+ (1.13 Å) [31]. The positive lithium effect is also confirmed by the existence of triple molybdates $A_3LiZn_2(MoO_4)_4$ (A=Rb, Cs) and $Cs_3LiCo_2(MoO_4)_4$ [9,10] isostructural to $Cs_6Zn_5(MoO_4)_8$. Another isostructural series of triple molybdates $A_3Li_2R(MoO_4)_4$ (sp. gr. $I\bar{4}2d$, Z=4) related to the $Cs_6Zn_5(MoO_4)_8$ structure and contained no cation vacancies was found in the systems A_2MoO_4–Li_2MoO_4–$R_2(MoO_4)_3$ (AR=RbAl, CsAl, TlAl, CsFe, CsGa, and RbGa) [10]. Due to a noticeable difference in sizes and charges of Li^+ and R^{3+}, these cations have the ordered arrangement in the compounds that lowers their symmetry. In both series, lithium ions, bivalent or trivalent cations completely fill vacancies in the Zn positions of the $Cs_6Zn_5(MoO_4)_8$-type structure, extending the unique structure type of double molybdates to the field of triple molybdates. The organizing role of lithium ions is exhibited also in the tetrahedral coordination of Co^{2+}, Al^{3+}, Fe^{3+}, and Ga^{3+} that is non-typical of those in molybdates and is far usual for Li^+. Taking into account a similar behavior of zinc cations, the combination of Li^+ and Zn^{2+} seems to be the most optimal variant for the stabilization of such structure as $Cs_6Zn_5(MoO_4)_8$.

4. Conclusion

A new sodium-containing member of the $Cs_6Zn_5(MoO_4)_8$ family, $Cs_3NaZn_2(MoO_4)_4$, was successfully prepared and its subsolidus phase relations in the Na_2MoO_4–Cs_2MoO_4–$ZnMoO_4$ system were studied at 420 °C. It was established that $Cs_3NaZn_2(MoO_4)_4$ is actually the end member of the continuous solid solution $Cs_6Zn_{5-x}\square_{1-x}Na_{2x}(MoO_4)_8$ ($0 \le x \le 1$) with a gradual insertion of Na^+ ions in vacancies of the tetrahedral Zn position of the $Cs_6Zn_5(MoO_4)_8$ structure following the scheme $Zn^{2+} + \square \rightarrow 2\,Na^+$. With increasing *the x* value, the cubic lattice parameter of the solid solution linearly increases while its melting point decreases that testifies to a destabilization of the $Cs_6Zn_5(MoO_4)_8$ structure by the insertion of Na^+. In fact, the existence region of the solid solution passes the limits of the $Cs_6Zn_5(MoO_4)_8$–$Cs_3NaZn_2(MoO_4)_4$ join and expands to the 2D area. In the $Cs_3NaZn_2(MoO_4)_4$ structure, MoO_4 and $(Zn_{2/3}Na_{1/3})O_4$ tetrahedra share vertices to form an open 3D framework. Cesium ions are found to be disordered around the centers of the cuboctahedral cavities of the framework to form "clusters" of the central Cs(1) and four disordered Cs(2) positions.

The melting points in the row $Cs_3NaZn_2(MoO_4)_4$ – $Cs_6Zn_5(MoO_4)_8$ – $Cs_3LiZn_2(MoO_4)_4$ are 510, 650, and 740 °C, respectively, that indicates the stabilizing effect of Li^+ ions on the $Cs_6Zn_5(MoO_4)_8$ structure in contrast to Na^+ ions. Thus, filling vacancies by foreign cations in the tetrahedral Zn position of the $Cs_6Zn_5(MoO_4)_8$ structure type would be better to perform with Li^+ ions as partners.

Upon studying the Na_2MoO_4–Cs_2MoO_4–$ZnMoO_4$ system, the boundary systems Na_2MoO_4–$ZnMoO_4$ and Na_2MoO_4–Cs_2MoO_4 were reinvestigated. The nonstoichiometric sodium zinc molybdates of the alluaudite and lyonsite types were found to have compositions $Na_{4-2x}Zn_{1+x}(MoO_4)_3$ ($0.1 \le x \le 0.4$) and $Na_{2-2y}Zn_{2+y}(MoO_4)_3$ ($0.1 \le y \le 0.2$) at 420 °C, respectively, whereas $Na_{2-2z}Zn_{2+z}(MoO_4)_3$ ($0.1 \le z \le 0.4$) isostructural to $Na_2Mg_5(MoO_4)_6$ exists above 550 °C only. The T–x phase diagram of the Na_2MoO_4–Cs_2MoO_4 system was also revised and hitherto unknown $Cs_3Na(MoO_4)_2$ was found. The compound has a reversible polymorphic transition at 390 °C and melts incongruently at 510 °C. The crystal structure of $Cs_3Na(MoO_4)_2$ was solved and found belonging to the glaserite type.

Ferroelastic properties revealed for glaserite-like low-temperature forms of $K_3Na(XO_4)_2$ (X=Se, Cr, Mo, and W) allow us to expect similar properties for $Cs_3Na(MoO_4)_2$. The disordered character of the $Cs_3NaZn_2(MoO_4)_4$ structure may also suggest lowering its symmetry at low temperatures with arising ferroelastic or ferroelectric properties. The studies are in progress.

Acknowledgments

The authors are grateful to Dr. Natalia V. Kuratieva, Dr. Irina A. Gudkova and Dr. Klara M. Khal'baeva for assistance in performing experiments and processing data. The authors thank Mrs. Tamara S. Yudanova for translating the paper from Russian. This work was partly supported by the Russian Foundation for Basic Research, Grant No. 14-03-00298.

Appendix A. Supplementary material

Supplementary data associated with this article can be found in the online version at http://dx.doi.org/10.1016/j.jssc.2015.10.008.

References

[1] P.V. Klevtsov, R.F. Klevtsova, Polymorphism of the double molybdates and tungstates of mono- and trivalent metals with the composition $M^+R^{3+}(EO_4)_2$,

J. Struct. Chem. 18 (1977) 339–355.
[2] V.A. Isupov, Binary molybdates and tungstates of mono- and trivalent elements as possible ferroelastics and ferroelectrics, Ferroelectrics 321 (2005) 63–90.
[3] V.A. Isupov, Ferroelectric and ferroelastic phase transitions in molybdates and tungstates of monovalent and bivalent elements, Ferroelectrics 322 (2005) 83–114.
[4] E.F. Dudnik, G.A. Kiosse, The structural peculiarities of some pure ferroelastics, Ferroelectrics. 48 (1983) 33–48.
[5] R.F. Klevtsova, S.F. Solodovnikov, P.V. Klevtsov, Structural changes during phase transition in ferroelastic $K_4Zn(MoO_4)_3$, Izvestiya Akademii Nauk SSSR. Seriya Fizicheskaya 50 (1986) 353–355 , in Russian.
[6] G. Nord, P. Kierkegaard, Statistics of divalent-metal coordination environments in inorganic oxide and oxosalts crystal-structures, Chem. Scr. 24 (1984) 151–158.
[7] S.F. Solodovnikov, P.V. Klevtsov, L.A. Glinskaya, R.F. Klevtsova, Synthesis and crystal structure of cesium zinc molybdate $Cs_6Zn_5(MoO_4)_8 = 2 \times Cs_3(Zn_{5/6}{}^{\square}{}_{1/6})_3(MoO_4)_4$, Kristallografiya 32 (1987) 618–622 , in Russian.
[8] M. Mueller, B.O. Hildmann, Th Hahn, Structure of $Cs_6Zn_5(MoO_4)_8$, Acta Crystallogr. C43 (1987) 184–186.
[9] Z.A. Solodovnikova, S.F. Solodovnikov, E.S. Zolotova, New triple molybdates $Cs_3LiCo_2(MoO_4)_4$ and $Rb_3LiZn_2(MoO_4)_4$, filled derivatives of the $Cs_6Zn_5(MoO_4)_8$ type, Acta Crystallogr. C62 (2006) 16–18.
[10] S.F. Solodovnikov, E.G. Khaikina, Z.A. Solodovnikova, Yu.M. Kadyrova, K. M. Khal'baeva, E.S. Zolotova, New families of lithium-containing triple molybdates and the stabilizing role of lithium in their structure formation, Dokl. Chem. 416 (2007) 207–212.
[11] R.G. Samuseva, R.M. Zharkova, V.E. Plyushchev, System of Na_2MoO_4–Cs_2MoO_4, Zhurnal Neorganicheskoi Khimii. 9 (1964) 2678–2679 , in Russian.
[12] V.P. Zueva, A.N. Shabanova, T.I. Drobasheva, Ternary system of Na_2MoO_4-Cs_2MoO_4-MoO_3, Zhurnal Neorganicheskoi Khimii. 27 (1982) 1599–1601 , in Russian.
[13] G.D. Tsyrenova, Z.G. Bazarova, M.V. Mokhosoev, Phase diagram of the $Cs_2MoO_4 - ZnMoO_4$ system, Zhurnal Neorganicheskoi Khimii. 33 (1988) 462–464 , in Russian.
[14] V.A. Efremov, V.K. Trunov, About double molybdates of alkali and divalent elements, Zhurnal Neorganicheskoi Khimii. 17 (1972) 2034–2039 , in Russian.
[15] V.A. Efremov, V.K. Trunov, The double tungstates and molybdates of alkali and some divalent elements, Neorg. Mater. 11 (1975) 273–277 , in Russian.
[16] V.A. Efremov, Y.A. Velikodnyi, V.K. Trunov, Crystal structures of $Na_{2.20}Zn_{0.90}(MoO_4)_2$ and $Na_5Sc(WO_4)_4$, Kristallografiya 20 (1975) 287–292 , in Russian.
[17] R.F. Klevtsova, V.G. Kim, P.V. Klevtsov, X-ray structural investigation of double molybdates $Na_2R_5{}^{2+}(MoO_4)_6$, R = Mg, Co and Zn, Kristallografiya 25 (1980) 1148–1154 , in Russian.
[18] C. Gicquel-Mayer, M. Mayer, Étude structurale du molybdate double $Na_{0.5}Zn_{2.75}(MoO_4)_3$, Rev. Chim. Miner. 19 (1982) 91–98.
[19] W. Guertler, Zur Fortentwicklung der Konstitutionsforschungen bei ternären Systemen, Z. Anorg. und Allg. Chem. 154 (1926) 439–455.
[20] L. Niepel, M. Malinovsky, Triangulation of phase diagrams, Chem. Zvesti. 32 (1978) 810–820.
[21] W. Kraus, G.J. Nolze, Powder cell – a program for the representation and manipulation of crystal structures and calculation of the resulting X-ray powder patterns, Appl. Cryst. 29 (1996) 301–303.
[22] G.M. Sheldrick, SHELX97, Release 97-2, Univ. of Göttingen, Göttingen, Germany, 1997.
[23] P.B. Moore, Crystal chemistry of the alluaudite structure type: contribution to the paragenesis of pegmatite phosphate giant crystals, Amer. Miner. 56 (1971) 1955–1975.
[24] J.M. Hughes, S.J. Starkey, M.L. Malinconico, L.L. Malinconico, Lyonsite, $Cu_3^{2+}Fe_4^{3+}(VO_4)_6^{3-}$, a new fumarolic sublimate from Izalco volcano, El Salvador: descriptive mineralogy and crystal structure, Amer. Miner. 72 (1987) 1000–1005.
[25] J. Fabry, V. Petricek, P. Vanek, I. Cisarova, Phase transition in $K_3Na(MoO_4)_2$ and determination of the twinned structures of $K_3Na(MoO_4)_2$ and $K_{2.5}Na_{1.5}(MoO_4)_2$ at room temperature, Acta Crystallogr. B53 (1997) 596–603.
[26] C. Bai, C. Lei, S. Pan, Y. Wang, Z. Yang, S. Han, H. Yu, Y. Yang, F. Zhang, Syntheses, structures and characterizations of $Rb_3Na(MO_4)_2$ (M = Mo, W) crystals, Solid State Sci. 33 (2014) 32–37.
[27] Y. Ding, N. Hou, N. Chen, Y. Xia, Phase diagrams of Li_2MoO_4–Na_2MoO_4 and Na_2MoO_4–K_2MoO_4 systems, Rare Metals 25 (2006) 316–320.
[28] M.V. Mokhosoev, K.M. Khal'baeva, E.G. Khaikina, A.M. Ogurtsov, Double sodium rubidium molybdates, Zhurnal Neorganicheskoi Khimii 35 (1990) 2126–2129 , in Russian.
[29] K. Okada, J. Ossaka, Structures of potassium sodium sulphate and tripotassium sodium disulphate, Acta Crystallogr. B. 36 (1980) 919–921.
[30] R. Nikolova, V. Kostov-Kytin, Crystal chemistry of "glaserite" type compounds, Bulg. Chem. Commun. 45 (2013) 418–426.
[31] R.D. Shannon, Revised effective ionic radii and systematic studies of interatomic distances in halides and chalcogenides, Acta Crystallogr. 32 (1976) 751–767.
[32] C. Gicquel-Mayer, M. Mayer, G. Perez, Etude stucturale du molybdate double $K_4Zn(MoO_4)_3$, Rev. Chim. Miner. 17 (1980) 445–457.
[33] W.T. Klooster, R.O. Piltz, T. Uda, S.M. Haile, Structure retinement and chemical analysis of $Cs_3Li(DSO_4)_4$, formerly '$_{1.5}Li_{1.5}D(SO_4)_2$', J. Solid State Chem. 177 (2004) 274–280.
[34] H. Bartl, Th Scheller, Zur Struktur des $12CaO \cdot 7Al_2O_3$, Neues Jahrb. Miner. Monatsh. 35 (1970) 547–552.
[35] P.P. Williams, Refinement of the structure of $11CaO \cdot 7Al_2O_3 \cdot CaF_2$, Acta Crystallogr. B29 (1973) 1550–1551.
[36] K. Tsukimura, Y. Kanazawa, M. Aoki, M. Bunno, Structure of wadalite $Ca_6Al_5Si_2O_{16}Cl_3$, Acta Crystallogr. C49 (1993) 205–207.
[37] I.E. Grey, I.C. Madsen, D.J. Jones, P.W. Smith, The structure of $Na_6Zn_3(AsO_4)_4 \cdot 3H_2O$ and its relationship to the garnet and other Ia3d-derived structures, J. Solid State Chem. 82 (1989) 52–59.
[38] V.A. Efremov, V.K. Trunov, T.A. Berezina, Delicate changes in the structure of scheelite-like $Na_5Tr(EO_4)_4$ during variations in their elemental composition, Kristallografiya 27 (1982) 134–139 , in Russian.
[39] E. Zintl, A. Harder, B. Dauth, Gitterstruktur der oxyde, sulfide, selenide und telluride des lithiums, natriums und kaliums, Z. Elektrochem. 40 (1934) 588–593.
[40] I.A. Grey, R.J. Hill, A.W. Hewat, A neutron powder diffraction study of the beta to gamma phase-transformation in $NaFeO_2$, Z. Kristallogr. 193 (1990) 51–69.
[41] J.A. Kaduk, S.-Y. Pei, The crystal-structure of hydrated sodium aluminate, $NaAlO_2 \cdot 5/4H_2O$, and its dehydratation product, J. Solid State Chem. 115 (1995) 126–139.
[42] J. Grins, L. Eriksson, Y. Kanno, The structure of one of the high-temperature modifications of Na_2ZnSiO_4, Solid State Ion. 92 (1996) 293–296.
[43] W.H. Baur, T. Ohta, R.D. Shannon, Structure of magnesium disodium silicate Na_2MgSiO_4 and ionic-conductivity in tetrahedral structures, Acta Crystallogr. B37 (1981) 1483–1491.